Topoisomerase I Essentiality, DnaA-independent Chromosomal Replication, and Transcription-Replication Conflict in *Escherichia coli*

J Krishna Leela[a], Nalini Raghunathan[a], and J Gowrishankar[a,b#]

[a]Laboratory of Bacterial Genetics, Centre for DNA Fingerprinting and Diagnostics, Hyderabad, India

[b]Indian Institute of Science Education and Research Mohali, SAS Nagar, India

Running Head: Topoisomerase I essentiality in *E. coli*

#Address correspondence to Dr J Gowrishankar (Orcid ID: 0000-0003-2483-9209), Tel: +91-172-2240266; Fax: +91-172-2240124; Email: shankar@iisermohali.ac.in

Keywords: DNA supercoiling, topoisomerase I, R-loops, constitutive stable DNA replication, transcription-replication conflict

Abstract

Topoisomerase I (Topo I) of *Escherichia coli*, encoded by *topA*, acts to relax negative supercoils in DNA. Topo I deficiency results in hypernegative supercoiling, formation of transcription-associated RNA-DNA hybrids (R-loops), and DnaA- and *oriC*-independent constitutive stable DNA replication (cSDR), but some uncertainty persists as to whether *topA* is essential for viability in *E. coli* and related enterobacteria. Here we show that several *topA* alleles, including Δ*topA*, confer lethality in derivatives of wild-type *E. coli* strain MG1655. Viability in absence of Topo I was restored with two perturbations, neither of which reversed the hypernegative supercoiling phenotype: (i) in a reduced-genome strain MDS42, or (ii) by an RNA polymerase (RNAP) mutation *rpoB*35* that has been reported to alleviate the deleterious consequences of RNAP backtracking and transcription-replication conflicts. Four phenotypes related to cSDR were identified for *topA* mutants: (i) One of the *topA* alleles rescued Δ*dnaA* lethality; (ii) in *dnaA*$^+$ derivatives, Topo I deficiency generated a characteristic copy number peak in the terminus region of the chromosome; (iii) *topA* was synthetically lethal with *rnhA* (encoding RNase HI, whose deficiency also confers cSDR); and (iv) *topA rnhA* synthetic lethality was itself rescued by Δ*dnaA*. We propose that the terminal lethal consequence of hypernegative DNA supercoiling in *E. coli topA* mutants is RNAP backtracking during transcription elongation and associated R-loop formation, which in turn lead to transcription-replication conflicts and to cSDR.

41 **Importance**

42 In all life forms, double helical DNA exists in a topologically supercoiled
43 state. The enzymes DNA gyrase and topoisomerase I act, respectively, to
44 introduce and to relax negative DNA supercoils in *Escherichia coli*. That gyrase
45 deficiency leads to bacterial death is well established, but the essentiality of
46 topoisomerase I for viability has been less certain. This study confirms that
47 topoisomerase I is essential for *E. coli* viability, and suggests that in its
48 absence aberrant chromosomal DNA replication and excessive transcription-
49 replication conflicts occur that are responsible for lethality.

50

Introduction

DNA in all cells is negatively supercoiled, and in bacteria such as *Escherichia coli* two enzymes gyrase and topoisomerase I (Topo I) ordinarily act oppositely to maintain the homeostasis of DNA superhelical density (reviewed in 1–4). DNA gyrase is a hetero-tetrameric enzyme (comprised of two subunits each of GyrA and GyrB proteins) that is ATP-dependent and introduces negative supercoils, whereas Topo I (encoded by *topA*) is an 865 amino acid-long monomer that catalyzes relaxation of supercoiled DNA in an energy-independent reaction. An important role for Topo I is in the dissipation of negative supercoils, in accord with the twin-domain supercoiling model (5, 6), that are generated behind RNA polymerase (RNAP) in the transcription elongation complex (TEC).

That gyrase deficiency leads to bacterial death is well established. On the other hand, the essentiality of Topo I for viability, in either *E. coli* or closely related bacteria such as *Salmonella enterica* and *Shigella flexneri*, is somewhat less certain (7–13). One difficulty has been that *topA* mutants rapidly accumulate suppressors which are often in the genes encoding the gyrase subunits (8–10, 13–17); and consistent with their opposing actions, gyrase and Topo I mutations can, in combination, partially cancel one another's sickness or inviability (18, 19). Growth of *E. coli topA* mutants is also improved upon overexpression or amplification of genes encoding the topoisomerases III (13, 18, 20) or –IV (10, 16, 19).

Topo I deficiency is associated with an increased prevalence of R-loops (RNA-DNA hybrids) in the cells, which has been attributed to re-annealing of the 5'-end of nascent RNA into hyper-negatively supercoiled DNA behind the TEC under these conditions (21–23, reviewed in 4, 24, 25). Overexpression of RNase HI (encoded by *rnhA*), which degrades RNA in RNA-DNA hybrids, can alleviate some of the phenotypes of *topA* mutants (18, 22, 23, 26–28); and conversely, *topA rnhA* mutants exhibit exacerbated sickness (13, 26, 29). In principle, R-loops can exert toxicity by acting as road-blocks to subsequent transcription (30, 31) and to replication (32–34); and a third mechanism for toxicity is by serving as sites for initiation of aberrant chromosomal

replication, as further outlined below. That R-loop formation is modulated by DNA supercoiling has been shown also in the CRISPR-Cas9 system (35), and in eukaryotic cells (36–38).

Recent evidence indicates that transcription-replication conflicts can themselves lead to increased formation of R-loops in the genome following RNAP backtracking at the sites of conflict (39–42, reviewed in 43–45). It has also been suggested that extended RNAP backtracking could be associated with R-loop formation from the 3'-end of the nascent RNA (40, 46).

R-loops are physiological initiators of ColE1 plasmid replication (47), but in addition their excessive occurrence (as in *rnhA* mutants) can lead to pathological initiation of chromosomal DNA replication in both bacteria (reviewed in 48–50) and eukaryotes (51). Such aberrant replication in bacteria is referred to as constitutive stable DNA replication (cSDR) since, unlike ordinary chromosomal replication which is initiated at *oriC* with the aid of the unstable protein DnaA, it continues long after inhibition of protein synthesis in the cells. cSDR can be identified biochemically as persistent DNA synthesis following addition of translational inhibitors such as chloramphenicol or spectinomycin.

cSDR can also be identified genetically as rescue of lethality associated with loss of DnaA function, which is a more stringent test of cSDR since it demonstrates the capability to duplicate the entire chromosome in the absence of *oriC*-initiated replication (48, 49). During its progression around the bacterial chromosome, such aberrant replication would be expected also to encounter (i) increased head-on conflicts with TECs on heavily transcribed genes (especially the *rrn* operons) that have evolved to be co-directional with *oriC*-initiated replisome progression, and (ii) increased arrest at *Ter* sites flanking the terminus region which are bound by the Tus protein (52, 53). The occurrence of cSDR in *rnhA* mutants has been established through both the biochemical and the genetic assays (48). The protein DksA, which participates in avoidance or resolution of transcription-replication conflicts (54, 55), is also required for viability of *rnhA dnaA* mutants (56).

In recent work, Drolet's group has shown by the biochemical assays that cSDR occurs in Topo I-deficient cells (28). Kornberg and coworkers had also shown earlier that specificity for replication initiation from *oriC in vitro* requires both RNase HI and Topo I (57, 58).

In this study, we have examined several *topA* insertion and deletion alleles for both their viability and their ability to rescue Δ*dnaA* lethality in *E. coli*. Our results indicate that *topA* null alleles are lethal in the wild-type strain MG1655 but that they are viable in MDS42, which is an engineered derivative lacking all prophages and transposable elements (59). The null mutants of MG1655 were viable with *rpoB*35*, which encodes an RNAP variant that has been reported to alleviate the deleterious effects of transcription-replication conflicts(40, 52, 60–65). Both in MDS42 and with *rpoB*35*, the viable Topo I-deficient derivatives continued to exhibit increased negative supercoiling. One *topA* allele could also rescue Δ*dnaA* lethality, providing genetic confirmation of cSDR in Topo I-deficient strains. We propose that bacterial lethality in absence of Topo I is caused by RNAP backtracking during transcription elongation and associated R-loop formation, which in turn then lead to transcription-replication conflicts and to cSDR.

Results

Description of *topA* insertion and deletion mutations and the assay to test for their viability. Three pairs of *topA* mutations were constructed on the *E. coli* chromosome by the recombineering approach of Datsenko and Wanner (66), each pair comprised of an FRT-flanked Kan^R element and the corresponding derivative with Flp recombinase-mediated site-specific excision of the Kan^R element to leave behind a "scar" of 27 in-frame codons; these are designated below by the suffixes "::Kan" and "::FRT", respectively.

The three pairs of mutations represent the following (Fig. 1A): (i) deletion of all but the first codon and the last six codons (860-865) of the *topA* open-reading frame (Δ*topA*), that is, similar to the various gene knock-outs of the Keio collection (67); (ii) insertion beyond codon 480 in *topA* (*topA*-Ins480), this position being chosen because an earlier study had shown that a Tet^R

insertion allele at this site was viable and associated with increased frequency of transposon precise excisions (11); and (iii) deletion beyond codon 480 until codon 860 in *topA* (*topA*-480Δ).

All the *topA* mutations were constructed and maintained in derivatives that were also Δ*lacZ* on the chromosome and carried a shelter plasmid derivative of a single-copy-number IncW replicon encoding trimethoprim (Tp)-resistance (68) with *topA*$^+$ and *lacZ*$^+$ genes. Since this plasmid's segregation into daughter cells during cell division is not tightly controlled, around 10% of cells in a population are plasmid-free. Only provided that these latter cells are viable, they grow as white colonies on Tp-free medium supplemented with Xgal, whereas the plasmid-bearing cells grow as blue colonies on these plates. The appearance of white colonies which can be subsequently purified, therefore, is a demonstration of viability in absence of the *topA*$^+$ shelter plasmid, and we have employed the similar blue-white screening assays earlier for tests of viability with other essential genes such as *rho*, *nusG*, *dnaA*, and *rne* (69–71).

Viability of *topA* mutations in MDS42 and MG1655 *rpoB*35*. With the blue-white assay above, we found that none of the six *topA* alleles is viable in MG1655 (Fig. 1B). These observations are consistent with those of Stockum et al. (13) who also employed a similar approach to conclude that *topA* is essential in *E. coli.*

By the same blue-white assay, we could show that all the *topA* mutations are viable in strain MDS42 and in *rpoB*35* derivatives of both MG1655 and MDS42, on both LB and defined media (Fig. 1B and Supp. Fig. S1A); the growth of white colonies of the MDS42 *topA* derivatives was improved in presence of *rpoB*35*, on both media (Supp. Fig. S1B). MDS42 is a derivative of MG1655 with 14% of its genome (comprising all prophages and transposable elements) deleted (59), while *rpoB*35* is a mutation in RNAP that has been reported to render the enzyme less prone to backtracking or arrest and more accommodative of conflicts with replication (40, 52, 60–65).

In microscopy experiments (Supp. Fig. S2), cell size and morphology

were unchanged with the *rpoB*35* mutation alone in both MG1655 and MDS42. Cells of the MDS42 *topA* mutant were filamented, and the filamentation was to a large extent suppressed in the *topA rpoB*35* derivative. The *topA rpoB*35* derivative of MG1655 was also moderately filamented.

Growth rate experiments in liquid cultures did not yield reliable data because of extended lag times and accumulation of suppressors in the *topA* derivatives. Suppressor accumulation has also been documented earlier for *topA* mutants by other workers (8, 13). Based on the observation that the "white" *topA* mutant clones in the blue-white screening assay grow to colonies of around 10^8 cells in 48 hours, we have estimated a doubling time of around 100 min.

For reasons that are explained in the Discussion, we tested whether suppression of *topA* lethality by *rpoB*35* in MG1655 is abolished in absence of the UvrD DNA helicase in the cells. In the blue-white assay, viable colonies of MG1655 *rpoB*35 topA* were obtained even in a Δ*uvrD* background, indicating that the suppression is UvrD-independent (Supp. Fig. S3A).

Rescue of *topA* lethality in MDS42 or by *rpoB*35* is not because of reversal of hypernegative supercoiling. Lethality caused by loss of Topo I is associated with greatly elevated levels of negative supercoiling *in vivo*, and at least some suppressors of inviability, such as mutations in *gyrA* or *gyrB* and overexpression or amplification of genes encoding topoisomerases III or -IV, also confer reversal of the hypernegative supercoiling phenotype. To examine whether the viability of *topA* null mutants in MDS42 and with *rpoB*35* is correlated with reversal of hypernegative supercoiling, we determined their supercoiling status, by chloroquine-agarose gel electrophoresis (21, 72) of a reporter plasmid pACYC184 (73) in preparations made from the different strain derivatives.

The results, shown in Figure 2, indicate that (i) in MDS42, both *topA* mutations tested confer increased supercoiling (compare lanes 3-6 with lanes 1-2); (ii) *rpoB*35* does not alter supercoiling, in both the *topA*$^+$ (compare within lane pairs 1 and 2, or 8 and 9) and *topA* derivatives (compare within lane pairs

3 and 4, or 5 and 6); and (iii) supercoiling levels are not different between the strain backgrounds of MG1655 and MDS42 for both *rpoB*$^+$ (compare lanes 1 and 8) and the *rpoB*35* mutant (compare lanes 2 and 9). We conclude that when lethality conferred by loss of Topo I is suppressed by either genome-size reduction in MDS42 or *rpoB*35*, or by both perturbations together, there is no concomitant reduction in the hypernegative supercoiling status of DNA in these mutants.

***topA* lethality in MG1655 is not rescued by ectopic expression of the R-loop helicase UvsW.** Ectopic expression of the phage T4-encoded R-loop helicase UvsW (74) has previously been shown to rescue lethality associated with increased R-loop prevalence in several different *E. coli* mutants. The latter include strains with combined deficiency of RNases HI and HII (69), or of RNase HI and RecG (75), as also those with deletions of genes *rho* or *nusG* involved in factor-dependent transcription termination (69).

Since Topo I deficiency phenotypes are also associated with increased occurrence of intracellular R-loops and are partially suppressed by RNase HI overexpression (18, 21–23, 26–28), we employed the blue-white assays to examine whether UvsW expression (from a P_{tac}-UvsW chromosomal construct, induced with IPTG) could rescue MG1655 *topA* lethality; an MG1655 Δ*rho* derivative (whose lethality is known to be rescued by UvsW) was chosen as control. The results indicate that UvsW expression does not confer viability to the MG1655 *topA* derivative, whereas it could do so to the Δ*rho* mutant (Supp. Fig. S3B). UvsW expression was associated with impaired growth of the *topA*$^+$ blue colonies; this growth impairment was exemplified both by a marked decrease in plating efficiency and by occurrence of blue haloes around the colonies, suggestive of cell lysis. That UvsW expression is toxic to wild-type *E. coli* has been reported earlier (69).

Rescue of Δ*dnaA* lethality by Topo I deficiency. As mentioned above, Topo I deficiency was earlier shown by a biochemical assay to confer cSDR, but whether it can rescue lethality associated with loss of DnaA function (that is, the genetic assay for cSDR) has not been determined. We adapted the blue-white assay to test whether any of the *topA* mutations can rescue lethality

associated with loss of DnaA function, by constructing a Tp^R *lacZ*$^+$ shelter plasmid that carried both *topA*$^+$ and *dnaA*$^+$. Three different *dnaA* alleles were used in these experiments: Δ*dnaA*::Kan (70), which is a Keio-style insertion-deletion that has removed all but the first codon and the last six codons of the 468-codon-long *dnaA* ORF; its FRT derivative, Δ*dnaA*::FRT (70); and *dnaA177* (76), whose DNA sequence determination revealed that it carries both a missense mutation in codon 267 (resulting in Thr-to-Ilv substitution) and an amber nonsense mutation in codon 450. The strains also carried Δ*tus* and *rpoB*35* mutations, which facilitate cSDR-directed chromosome duplication by overcoming the problems posed, respectively, by the *Ter* sites and by excessive head-on transcription-replication conflicts (52, 70, 77, 78).

Of the six *topA* mutations tested that had been shown above to be lethal in MG1655, one (*topA*-Ins480::FRT) was able to rescue lethality of Δ*dnaA*::FRT and of *dnaA177* at 30° on both minimal and LB media (Fig. 3A-B and Supp. Fig. S4A), while the others yielded no viable white colonies (Fig. 3A). Even with *topA*-Ins480::FRT, there was no rescue imposed by DnaA deficiency at 37° or 42° (Fig. 3B, see also row 5 in each of the panels of Supp. Fig. S5), nor were viable colonies recovered with the Δ*dnaA*::Kan allele (Fig. 3A). On the other hand, Δ*dnaA*::Kan lethality is rescued by other cSDR-provoking mutations such as *rnhA* or *dam* (data not shown).

Two distinct and interesting interpretations are suggested from these data: (i) that unlike the other five *topA* alleles, *topA*-Ins480::FRT might possess a low level of DNA relaxation activity (since it encodes a full-length polypeptide with just a 27-amino acid linker inserted between residues 480 and 481 of Topo I) which is not sufficient for viability *per se* in MG1655 but nonetheless is necessary for viability in the derivatives whose sole source of chromosome duplication is cSDR; and (ii) that expression of the essential *dnaN* gene immediately downstream of, and in the same operon as, *dnaA* is achieved from a fortuitous outward reading promoter in the Kan^R element of the Δ*dnaA*::Kan allele, but that this promoter is rendered inactive under TopoI-deficient conditions.

Notwithstanding these unusual features, our data clearly establish that

cSDR in a Topo I-deficient derivative can act to rescue the lethality associated with total absence of DnaA in the cells. This viability is contingent on absence of the Tus protein (Supp. Fig. S4B). On the other hand, the DinG helicase, which has been shown to be needed for Δ*dnaA* viability of RecG- or Dam-deficient cells (70), was not so required in the Topo I-deficient strain, nor did its absence impede viability of the *topA* mutant in the *dnaA*$^+$ derivative (Supp. Fig. S4C).

Copy number analysis of different chromosomal regions in *topA* mutants. In an exponentially growing population of bacterial cells, DnaA-initiated replication imposes a bidirectional gradient of copy number for different regions of the circular chromosome, with the peak near *oriC* and trough in the terminus region (53). If a *dnaA*$^+$ strain also suffers a perturbation that activates cSDR (such as deficiency of RNase HI, RecG, Dam, or multiple DNA exonucleases), the DNA copy number pattern is characterized by superposition of a "mid-terminus peak" on the bidirectional gradient described above (52, 70, 77–82). We have earlier proposed that the mid-terminus peak represents a population aggregate of replication forks progressing from stochastically firing cSDR origins that are widely distributed across the genome (53, 70), although other groups have suggested that it represents a discrete origin of replication (52, 77–79), or occurrence of over-replication when oppositely directed forks converge at the terminus (80, 81).

Drolet and coworkers have shown earlier that Topo I-deficient mutants exhibit the mid-terminus peak (19), but their strains also carried additional genetic changes such as a *gyrB* (Ts) mutation and amplification of the genes encoding subunits of topoisomerase IV. For our DNA copy number analysis studies, we used *dnaA*$^+$ strains of the MDS42 background without or with *rpoB*35* and additionally with the *topA*-Ins480::FRT mutation (that is, the allele associated with rescue of Δ*dnaA* inviability).

The whole genome sequence reads obtained from each of the strains were aligned to the MDS42 reference sequence, and normalized read counts for the different chromosomal regions were determined. No suppressor mutation in any of the candidate genes was identified in the *topA* mutants,

while presence of the *topA* mutation itself and of the CAC-to-CAA codon change (His-to-Gln substitution) associated with the *rpoB*35* allele (60) was confirmed in each of the relevant strains.

The parental (*topA*$^+$ *rpoB*$^+$) strain exhibited the expected bidirectional copy number gradient from *oriC* to *Ter* (Fig. 4, panel i), which was also largely preserved in its *rpoB*35* derivative (Fig. 4, panel ii). The *topA* mutant derivatives of both these strains showed distinct mid-terminus peaks superimposed on the *oriC*-to-*Ter* gradient (Fig. 4, panels iii and iv, respectively).

These results therefore confirm that a *topA* mutation capable of conferring Δ*dnaA* viability is associated with a mid-terminus peak of DNA copy number in *dnaA*$^+$ derivatives.

Mutual suppression between lethal mutations: loss of DnaA suppresses *topA*-*rnhA* synthetic lethality. Deficiency of either Topo I or RNase HI is associated with cSDR, and Stockum et al. (13) as well as Drolet and coworkers (26, 29) have earlier reported lethality or aggravated sickness in the double-deficient strains. We too found in this study that introduction of the *rnhA* mutation into otherwise viable *topA* derivatives (that is, in the MG1655-derived strain with *rpoB*35* and Δ*tus* mutations) confers synthetic lethality; the two *topA* alleles tested were the FRT derivatives of *topA*-Ins480 and Δ*topA* (Fig. 5, compare panels i-ii for former, and iv-v for latter). The lethalities were rescued in presence of Δ*dnaA* (Fig. 5, panels iii and vi, respectively), indicating that two otherwise lethal mutant combinations (*topA rnhA* and *dnaA*) could mutually suppress one another. Robust viability of the triple mutants was observed on both rich and defined media at 30° and 37°, less so at 42° (Supp. Fig. S5).

We performed PCR experiments to confirm that the chromosomal *topA* locus in each of the viable triple mutant *topA rnhA dnaA* derivatives was indeed disrupted (and had not, for example, become *topA*$^+$ by gene conversion from the wild-type allele on the shelter plasmid). Two primer pairs were used simultaneously to distinguish between the *topA*$^+$, Δ*topA*::FRT, and *topA*-

Ins480::FRT alleles, that yielded amplicons of 500, 328, and 581 bp, respectively (Supp. Fig. S6A-B). The results established that the signatures for the *topA*-Ins480 and Δ*topA* mutations were present, and that for *topA*$^{+}$ was absent, in the triple mutant strains (Supp. Fig. S6B, lanes 5 and 7, respectively).

As discussed below, these results suggest that it is excessive chromosomal replication which kills cells doubly defective for Topo I and RNase HI.

Discussion

The enzymes Topo I and DNA gyrase act to maintain the homeostatic balance of DNA negative supercoiling in *E. coli*. Topo I relaxes negative supercoils, especially those occurring behind RNAP during transcription elongation, and thus prevents the nascent transcript from re-annealing with the template DNA strand to form R-loops.

In this study, we have confirmed that Topo I-deficient *E. coli* mutants are inviable, and furthermore have identified two novel means by which the lethality can be independently and additively suppressed: (i) by deletion of the non-essential 14% of the genome comprising prophages and transposable elements, as in the strain MDS42; and (ii) by the *rpoB*35* mutation encoding an altered RNAP which has earlier been variously described (not mutually exclusive) to mimic the transcriptional effects of ppGpp (60), to reduce RNAP backtracking (40), and to mitigate the effects of transcription-replication conflicts by destabilizing the TEC (40, 52, 62, 63, 65). Neither of the suppressors acts by reversing hypernegative supercoiling in the *topA* mutants. We have also shown that Topo I deficiency, in the presence of additional *rpoB*35* and Δ*tus* mutations, can rescue Δ*dnaA* lethality, thereby providing genetic confirmation for occurrence of cSDR in the Topo I-deficient derivatives.

***rpoB*35* and RNAP backtracking.** As mentioned above, several workers have provided evidence that the *rpoB*35*-encoded substitution in RNAP destabilizes the TEC in vitro (40, 62) and protects against transcription-replication

conflicts in vivo (65), including during cSDR (52, 70, 77, 78). Trautinger and Lloyd (61) have reported that *rpoB*35* suppresses the Ts phenotype of *greA greB* double mutants and the UV-sensitivity of an *mfd* mutant, which they interpret as evidence that it may function by preventing backtracking, thus facilitating dissociation of stalled TECs. Likewise, *rpoB*35* also suppresses *rep uvrD* lethality, which has been ascribed to direct reduction of replicative barriers posed by TECs under these conditions (63).

On the other hand, there is one report from the Nudler group that RpoB*35-substituted RNAP exhibits increased backtracking in vitro in presence of UvrD (64). This property of RpoB*35-RNAP appears to be strictly UvrD-dependent, and the same group has shown in other studies (40) that relative to wild-type RNAP, the RpoB*35 enzyme is resistant to pausing and backtracking.

It is therefore reasonable to conclude that the RpoB*35 enzyme is in general more resistant than wild-type RNAP to arrest and backtracking during transcription elongation, except perhaps in the specific context when a high concentration of UvrD dimers occurs following DNA damage. Our finding in this study, that the suppression of *topA* lethality by *rpoB*35* is UvrD-independent (Supp. Fig. S3A), is noteworthy in this context.

Mechanism of lethality in Topo I-deficient strains. The fact that *rpoB*35* restores growth to MG1655 in absence of Topo I without affecting the hypernegative supercoiling status of the mutants suggests that it is the downstream consequences of increased negative supercoiling, namely RNAP backtracking and impairment of TEC progression leading to transcription-replication conflicts, which are responsible for *topA* lethality. Pathological R-loop formation is also expected to be an important feature at the arrested TECs, but whether it precedes or follows RNAP backtracking remains to be determined. In the *topA* mutant, *rpoB*35* would also relieve the sickness during cSDR engendered by transcription-replication conflicts especially at the *rrn* operons.

To explain *topA* viability in MDS42, we propose that the regions of the genome that are deleted in this strain (comprising prophages and transposable elements) are preferentially enriched for sites of R-loop formation, TEC arrest and transcription-replication conflict. Loss of the proteins Rho or NusG, that are involved in factor-dependent transcription termination and reportedly in R-loop avoidance (31, 69, 83-85), is also better tolerated in MDS42 than in MG1655, and especially so in presence of *rpoB*35* (65, 69, 86).

Finally, why does ectopic expression of the R-loop helicase UvsW not rescue *topA* lethality, although it can rescue the lethalities associated with loss of RNase H enzymes, RecG, Rho or NusG (69, 75)? One possibility is that R-loop formation in Topo I-deficient strains is a consequence, and not cause, of RNAP backtracking and arrest, so that R-loop removal per se would not mitigate the primary problem. An alternative possibility is that Topo I itself is required to relax the negative supercoils arising from UvsW's helicase action on R-loops, and hence that UvsW is unable to act efficiently to unwind R-loops specifically in the *topA* mutants. The fact that RNase HI overexpression can suppress *topA* sickness phenotypes (26, 27) lends support to the second model.

Topo I deficiency and cSDR. Drolet and coworkers had provided biochemical evidence for cSDR in Topo I-deficient cultures (28), which is presumably initiated from R-loops in these cells; our data establish that such cSDR is sufficient to sustain viability in absence of DnaA, in derivatives carrying Δ*tus* and *rpoB*35* mutations. The latter two mutations are expected to facilitate the completion of replication of the circular chromosome by forks initiated from site(s) other than *oriC* (52, 70, 77, 78). Our data also support the earlier suggestion (70) that incubation at 30° is more permissive than that at 37° or 42° for rescue by cSDR of Δ*dnaA* lethality.

Of the six different *topA* mutations that were inviable in MG1655-derived strains, it was only the *topA*-Ins480::FRT allele that could confer viability to the Δ*dnaA* derivatives. As explained above, this mutation generates a modified version of Topo I in which a 27 amino acid-linker is inserted

between residues 480 and 481 of the polypeptide. From the Topo I monomer crystal structure (87, 88), it is expected that the linker is situated at or near the junction between residues that comprise domain D2 and those that comprise domain D4; it is therefore possible that the linker may allow for (the albeit inefficient) folding of the polypeptide to yield a correct tertiary structure. The residual Topo I activity of this protein might be needed for proper chromosome segregation after cSDR in the Δ*dnaA* mutants (20).

***oriC*-initiated replication contributes to *topA-rnhA* synthetic lethality.** We have shown that although the Δ*topA* and Δ*rnhA* combination is synthetically lethal, the Δ*topA* Δ*rnhA* Δ*dnaA* mutant is viable. Thus, *oriC*-initiated replication is a contributor to *topA rnhA* toxicity, which suggests that it is excessive replication (sum of that from *oriC* and cSDR, the latter contributed additively by both *rnhA* and *topA*) which confers toxicity. These results are in agreement with those from Drolet and coworkers (20, 29), who had earlier reported that mutations affecting either replication from *oriC* or replication restart functions can alleviate the sickness of cells deficient for both Topo I and RNase HI activities.

Materials and Methods

Growth media, bacterial strains and plasmids. The rich and defined growth media were, respectively, LB and minimal A with 0.2% glucose (89) and, unless otherwise indicated, the growth temperature was 37°. Supplementation with Xgal and with antibiotics ampicillin, kanamycin (Kan), tetracycline (Tet), chloramphenicol (Cm), and trimethoprim (Tp) were at the concentrations described earlier (90). Isopropyl-β-D-thiogalactoside (IPTG) was added at the indicated concentrations. *E. coli* strains used are listed in Table S1, in the supplemental material.

Plasmids described earlier include pMU575 (Tp^R, single-copy-number vector with *lacZ*$^+$) (68); pACYC184 (Tet^R Cm^R, p15A replicon) (73); pHYD2388 (70) and pHYD2411 (69) (Tp^R, pMU575 derivatives with, respectively, *dnaA*$^+$ and *rho*$^+$); and pKD13, pKD46 and pCP20 described by Datsenko and Wanner (66) for recombineering experiments and Flp-recombinase catalyzed excision between a pair of FRT sites. The construction of two derivatives of plasmid

pMU575 is described in the supplemental material: pHYD2382, carrying *topA*$^+$, and pHYD2390, carrying *topA*$^+$ *dnaA*$^+$.

Blue-white screening assays. To determine lethality or viability of strains with chromosomal *topA* or *dnaA* mutations, derivatives carrying the shelter plasmids pHYD2382 (*topA*$^+$) or pHYD2390 (*topA*$^+$ *dnaA*$^+$) were grown overnight in Tp-supplemented medium, subcultured into medium without Tp for growth to mid-exponential phase, and plated at suitable dilutions on Xgal plates without Tp. The percentage of white colonies to total was determined (minimum of 500 colonies counted), and representative images were captured.

Plasmid supercoiling assays. Strains carrying plasmid pACYC184 were grown in LB to mid-exponential phase, and plasmid preparations were made with the aid of a commercial kit. Plasmid supercoiling status in each of the preparations was determined essentially as described (72), following electrophoresis on 1% agarose gel with 5 μg/ml chloroquine at 3 V/cm for 17 hr.

Copy number analysis by deep sequencing. Copy number determinations of the various genomic regions were performed essentially as described (70). Genomic DNA was extracted by the phenol-chloroform method from cultures grown in LB to mid-exponential phase, and single-end deep sequencing was performed on Illumina platforms to achieve around 100-fold coverage for each preparation. Sequence reads were aligned to the MDS42 reference genome (Accession number NC_020518.1), and copy numbers were then determined by a moving-average method after normalization of the base read count for each region to the aggregate of aligned base read counts for that culture.

Other methods. Procedures were as described for P1 transduction (91) and for recombinant DNA manipulations, PCR, and transformation (92). Different chromosomal *topA* mutations were generated by recombineering (66) as described in the supplemental material. For microscopy experiments, cells from cultures grown in LB to mid-exponential phase were immobilized on 1% agarose pads and visualized by differential interference contrast imaging with the aid of a Zeiss Axio Imager Z2 microscope.

Data availability. Genome sequence data from this work have been

491 submitted under Accession number PRJNA670792 and are available for
492 public access at https://www.ncbi.nlm.nih.gov/Traces/study/?acc=PRJNA670792 .

493 **Supplemental material**

494 Supplemental material is provided as a PDF file "Supplemental File 1".

495 **Acknowledgements**

496 We thank Jillella Mallikarjun for sequencing the *dnaA177* allele; Aswin
497 Seshasayee and T V Reshma for help with deep sequencing; V Balaji for
498 assistance with microscopy; and the COE team members for advice and
499 discussions.

500 This work was supported by Government of India funds from (i) DBT
501 Centre of Excellence (COE) project for Microbial Biology – Phase 2, (ii) SERB
502 project CRG/2018/000348, and (iii) DBT project
503 BT/PR34340/BRB/10/1815/2019. JG was recipient of the J C Bose
504 fellowship and INSA Senior Scientist award.

505 We declare that there are no conflicts of interest.

506 **References**

507 1. Vos SM, Tretter EM, Schmidt BH, Berger JM. 2011. All tangled up: how
508 cells direct, manage and exploit topoisomerase function. Nat Rev Mol
509 Cell Biol 12:827–841.
510 2. Chen SH, Chan NL, Hsieh TS. 2013. New mechanistic and functional
511 insights into DNA topoisomerases. Annu Rev Biochem 82:139–170.
512 3. Bush NG, Evans-Roberts K, Maxwell A. 2015. DNA topoisomerases.
513 EcoSal Plus doi:10.1128/ecosalplus.ESP-0010-2014.
514 4. Brochu J, Breton E V, Drolet M. 2020. Supercoiling, R-loops, Replication
515 and the Functions of Bacterial Type 1A Topoisomerases. Genes 11:pli-
516 E249.
517 5. Liu LF, Wang JC. 1987. Supercoiling of the DNA template during
518 transcription. Proc Natl Acad Sci U S A 84:7024–7027.
519 6. Dorman CJ. 2019. DNA supercoiling and transcription in bacteria: a
520 two-way street. BMC Mol cell Biol 20:26.
521 7. Sternglanz R, DiNardo S, Voelkel KA, Nishimura Y, Hirota Y, Becherer

K, Zumstein L, Wang JC. 1981. Mutations in the gene coding for *Escherichia coli* DNA topoisomerase I affect transcription and transposition. Proc Natl Acad Sci U S A 78:2747–2751.

8. Richardson SM, Higgins CF, Lilley DM. 1984. The genetic control of DNA supercoiling in *Salmonella typhimurium*. EMBO J 3:1745–1752.
9. Ni Bhriain N, Dorman CJ. 1993. Isolation and characterization of a *topA* mutant of *Shigella flexneri*. Mol Microbiol 7:351–358.
10. McNairn E, Ni Bhriain N, Dorman CJ. 1995. Overexpression of the *Shigella flexneri* genes coding for DNA topoisomerase IV compensates for loss of DNA topoisomerase I: effect on virulence gene expression. Mol Microbiol 15:507–517.
11. Reddy M, Gowrishankar J. 1997. Identification and characterization of *ssb* and *uup* mutants with increased frequency of precise excision of transposon Tn*10* derivatives: nucleotide sequence of *uup* in *Escherichia coli*. J Bacteriol 179:2892–2899.
12. Stupina VA, Wang JC. 2005. Viability of *Escherichia coli topA* mutants lacking DNA topoisomerase I. J Biol Chem 280:355–360.
13. Stockum A, Lloyd RG, Rudolph CJ. 2012. On the viability of *Escherichia coli* cells lacking DNA topoisomerase I. BMC Microbiol 12:26.
14. DiNardo S, Voelkel KA, Sternglanz R, Reynolds AE, Wright A. 1982. *Escherichia coli* DNA topoisomerase I mutants have compensatory mutations in DNA gyrase genes. Cell 31:43–51.
15. Pruss GJ, Manes SH, Drlica K. 1982. *Escherichia coli* DNA topoisomerase I mutants: increased supercoiling is corrected by mutations near gyrase genes. Cell 31:35–42.
16. Raji A, Zabel DJ, Laufer CS, Depew RE. 1985. Genetic analysis of mutations that compensate for loss of *Escherichia coli* DNA topoisomerase I. J Bacteriol 162:1173–1179.
17. Zhu Q, Pongpech P, DiGate RJ. 2001. Type I topoisomerase activity is required for proper chromosomal segregation in *Escherichia coli*. Proc Natl Acad Sci U S A 98:9766–9771.
18. Broccoli S, Phoenix P, Drolet M. 2000. Isolation of the *topB* gene encoding DNA topoisomerase III as a multicopy suppressor of *topA* null

555 mutations in *Escherichia coli*. Mol Microbiol 35:58–68.
556 19. Brochu J, Vlachos-Breton E, Sutherland S, Martel M, Drolet M. 2018.
557 Topoisomerases I and III inhibit R-loop formation to prevent unregulated
558 replication in the chromosomal Ter region of *Escherichia coli*. PLoS Genet
559 14:e1007668.
560 20. Usongo V, Drolet M. 2014. Roles of type 1A topoisomerases in genome
561 maintenance in *Escherichia coli*. PLoS Genet 10:e1004543.
562 21. Drolet M, Bi X, Liu LF. 1994. Hypernegative supercoiling of the DNA
563 template during transcription elongation *in vitro*. J Biol Chem 269:2068–
564 2074.
565 22. Masse E, Phoenix P, Drolet M. 1997. DNA topoisomerases regulate R-
566 loop formation during transcription of the *rrnB* operon in *Escherichia*
567 *coli*. J Biol Chem 272:12816–12823.
568 23. Masse E, Drolet M. 1999. *Escherichia coli* DNA topoisomerase I inhibits
569 R-loop formation by relaxing transcription-induced negative
570 supercoiling. J Biol Chem 274:16659–16664.
571 24. Drolet M. 2006. Growth inhibition mediated by excess negative
572 supercoiling: the interplay between transcription elongation, R-loop
573 formation and DNA topology. Mol Microbiol 59:723–730.
574 25. Belotserkovskii BP, Tornaletti S, D'Souza AD, Hanawalt PC. 2018. R-
575 loop generation during transcription: Formation, processing and cellular
576 outcomes. DNA Repair (Amst) 71:69–81.
577 26. Drolet M, Phoenix P, Menzel R, Masse E, Liu LF, Crouch RJ. 1995.
578 Overexpression of RNase H partially complements the growth defect of
579 an *Escherichia coli* delta *topA* mutant: R-loop formation is a major
580 problem in the absence of DNA topoisomerase I. Proc Natl Acad Sci U S
581 A 92:3526–3530.
582 27. Masse E, Drolet M. 1999. R-loop-dependent hypernegative supercoiling
583 in *Escherichia coli topA* mutants preferentially occurs at low
584 temperatures and correlates with growth inhibition. J Mol Biol 294:321–
585 332.
586 28. Martel M, Balleydier A, Sauriol A, Drolet M. 2015. Constitutive stable
587 DNA replication in *Escherichia coli* cells lacking type 1A topoisomerase

588 activity. DNA Repair (Amst) 35:37–47.
589 29. Usongo V, Martel M, Balleydier A, Drolet M. 2016. Mutations reducing
590 replication from R-loops suppress the defects of growth, chromosome
591 segregation and DNA supercoiling in cells lacking topoisomerase I and
592 RNase HI activity. DNA Repair (Amst) 40:1–17.
593 30. Hraiky C, Raymond MA, Drolet M. 2000. RNase H overproduction
594 corrects a defect at the level of transcription elongation during rRNA
595 synthesis in the absence of DNA topoisomerase I in *Escherichia coli*. J
596 Biol Chem 275:11257–11263.
597 31. Raghunathan N, Kapshikar RM, Leela JK, Mallikarjun J, Bouloc P,
598 Gowrishankar J. 2018. Genome-wide relationship between R-loop
599 formation and antisense transcription in *Escherichia coli*. Nucleic Acids
600 Res 46:3400–3411.
601 32. Gan W, Guan Z, Liu J, Gui T, Shen K, Manley JL, Li X. 2011. R-loop-
602 mediated genomic instability is caused by impairment of replication fork
603 progression. Genes Dev 25:2041–2056.
604 33. Gómez-González B, Aguilera A. 2019. Transcription-mediated
605 replication hindrance: A major driver of genome instability. Genes Dev.
606 33:1008–1026.
607 34. Garcia-Muse T, Aguilera A. 2019. R Loops: From Physiological to
608 Pathological Roles. Cell 179:604–618.
609 35. Ivanov IE, Wright A V, Cofsky JC, Aris KDP, Doudna JA, Bryant Z. 2020.
610 Cas9 interrogates DNA in discrete steps modulated by mismatches and
611 supercoiling. Proc Natl Acad Sci U S A 117:5853–5860.
612 36. El Hage A, French SL, Beyer AL, Tollervey D. 2010. Loss of
613 Topoisomerase I leads to R-loop-mediated transcriptional blocks during
614 ribosomal RNA synthesis. Genes Dev 24:1546–1558.
615 37. Tuduri S, Crabbe L, Conti C, Tourriere H, Holtgreve-Grez H, Jauch A,
616 Pantesco V, De Vos J, Thomas A, Theillet C, Pommier Y, Tazi J, Coquelle
617 A, Pasero P. 2009. Topoisomerase I suppresses genomic instability by
618 preventing interference between replication and transcription. Nat Cell
619 Biol 11:1315–1324.
620 38. Zhang T, Wallis M, Petrovic V, Challis J, Kalitsis P, Hudson DF. 2019.

621 Loss of TOP3B leads to increased R-loop formation and genome
622 instability. Open Biol 9:190222.
623 39. Boubakri H, de Septenville AL, Viguera E, Michel B. 2010. The helicases
624 DinG, Rep and UvrD cooperate to promote replication across
625 transcription units *in vivo*. EMBO J 29:145–157.
626 40. Dutta D, Shatalin K, Epshtein V, Gottesman ME, Nudler E. 2011.
627 Linking RNA polymerase backtracking to genome instability in *E. coli*.
628 Cell 146:533–543.
629 41. Lang KS, Hall AN, Merrikh CN, Ragheb M, Tabakh H, Pollock AJ,
630 Woodward JJ, Dreifus JE, Merrikh H. 2017. Replication-transcription
631 conflicts generate R-loops that orchestrate bacterial ctress survival and
632 pathogenesis. Cell 170:787-799.
633 42. Hamperl S, Bocek MJ, Saldivar JC, Swigut T, Cimprich KA. 2017.
634 Transcription-replication conflict orientation modulates R-loop levels
635 and activates distinct DNA damage responses. Cell 170:774-786.
636 43. Nudler E. 2012. RNA polymerase backtracking in gene regulation and
637 genome instability. Cell 149:1438–1445.
638 44. Lang KS, Merrikh H. 2018. The clash of macromolecular titans:
639 replication-transcription conflicts in bacteria. Annu Rev Microbiol
640 72:71–88.
641 45. Kuzminov A. 2018. When DNA topology turns deadly - RNA polymerases
642 dig in their R-loops to stand their ground: new positive and negative
643 (super)twists in the replication-transcription conflict. Trends Genet
644 34:111–120.
645 46. Zatreanu D, Han Z, Mitter R, Tumini E, Williams H, Gregersen L, Dirac-
646 Svejstrup AB, Roma S, Stewart A, Aguilera A, Svejstrup JQ. 2019.
647 Elongation factor TFIIS prevents transcription stress and R-loop
648 accumulation to maintain genome stability. Mol Cell 76:57-69.
649 47. Itoh T, Tomizawa J. 1980. Formation of an RNA primer for initiation of
650 replication of ColE1 DNA by ribonuclease H. Proc Natl Acad Sci U S A
651 77:2450–2454.
652 48. Kogoma T. 1997. Stable DNA replication: interplay between DNA
653 replication, homologous recombination, and transcription. Microbiol

Mol Biol Rev 61:212–238.

49. Drolet M, Brochu J. 2019. R-loop-dependent replication and genomic instability in bacteria. DNA Repair (Amst) 84:102693.
50. Sinha AK, Possoz C, Leach DRF. 2020. The roles of bacterial DNA double-strand break repair proteins in chromosomal DNA replication. FEMS Microbiol Rev 44:351–368.
51. Stuckey R, Garcia-Rodriguez N, Aguilera A, Wellinger RE. 2015. Role for RNA:DNA hybrids in origin-independent replication priming in a eukaryotic system. Proc Natl Acad Sci U S A 112:5779–5784.
52. Rudolph CJ, Upton AL, Stockum A, Nieduszynski CA, Lloyd RG. 2013. Avoiding chromosome pathology when replication forks collide. Nature 500:608–611.
53. Gowrishankar J. 2015. End of the beginning: elongation and termination features of alternative modes of chromosomal replication initiation in bacteria. PLoS Genet11:e1004909.
54. Tehranchi AK, Blankschien MD, Zhang Y, Halliday JA, Srivatsan A, Peng J, Herman C, Wang JD. 2010. The transcription factor DksA prevents conflicts between DNA replication and transcription machinery. Cell 141:595–605.
55. Zhang Y, Mooney RA, Grass JA, Sivaramakrishnan P, Herman C, Landick R, Wang JD. 2014. DksA guards elongating RNA polymerase against ribosome-stalling-induced arrest. Mol Cell 53:766–778.
56. Myka KK, Kusters K, Washburn R, Gottesman ME. 2019. DksA-RNA polymerase interactions support new origin formation and DNA repair in *Escherichia coli*. Mol Microbiol 111:1382–1397.
57. Ogawa T, Pickett GG, Kogoma T, Kornberg A. 1984. RNase H confers specificity in the dnaA-dependent initiation of replication at the unique origin of the *Escherichia coli* chromosome *in vivo* and *in vitro*. Proc Natl Acad Sci U S A 81:1040–1044.
58. Kaguni JM, Kornberg A. 1984. Topoisomerase I confers specificity in enzymatic replication of the *Escherichia coli* chromosomal origin. J Biol Chem 259:8578–8583.
59. Posfai G, Plunkett 3rd G, Feher T, Frisch D, Keil GM, Umenhoffer K,

687 Kolisnychenko V, Stahl B, Sharma SS, de Arruda M, Burland V, Harcum
688 SW, Blattner FR. 2006. Emergent properties of reduced-genome
689 *Escherichia coli*. Science 312:1044–1046.
690 60. McGlynn P, Lloyd RG. 2000. Modulation of RNA polymerase by (p)ppGpp
691 reveals a RecG-dependent mechanism for replication fork progression.
692 Cell 101:35–45.
693 61. Trautinger BW, Lloyd RG. 2002. Modulation of DNA repair by mutations
694 flanking the DNA channel through RNA polymerase. EMBO J 21:6944–
695 6953.
696 62. Trautinger BW, Jaktaji RP, Rusakova E, Lloyd RG. 2005. RNA
697 polymerase modulators and DNA repair activities resolve conflicts
698 between DNA replication and transcription. Mol Cell 19:247–258.
699 63. Guy CP, Atkinson J, Gupta MK, Mahdi AA, Gwynn EJ, Rudolph CJ,
700 Moon PB, van Knippenberg IC, Cadman CJ, Dillingham MS, Lloyd RG,
701 McGlynn P. 2009. Rep provides a second motor at the replisome to
702 promote duplication of protein-bound DNA. Mol Cell 36:654–666.
703 64. Kamarthapu V, Epshtein V, Benjamin B, Proshkin S, Mironov A, Cashel
704 M, Nudler E. 2016. ppGpp couples transcription to DNA repair in *E. coli*.
705 Science 352:993–996.
706 65. Washburn RS, Gottesman ME. 2011. Transcription termination
707 maintains chromosome integrity. Proc Natl Acad Sci U S A 108:792–797.
708 66. Datsenko KA, Wanner BL. 2000. One-step inactivation of chromosomal
709 genes in *Escherichia coli* K-12 using PCR products. Proc Natl Acad Sci U
710 S A 97:6640–6645.
711 67. Baba T, Ara T, Hasegawa M, Takai Y, Okumura Y, Baba M, Datsenko
712 KA, Tomita M, Wanner BL, Mori H. 2006. Construction of *Escherichia*
713 *coli* K-12 in-frame, single-gene knockout mutants: the Keio collection.
714 Mol Syst Biol 2:2006 0008.
715 68. Andrews AE, Lawley B, Pittard AJ. 1991. Mutational analysis of
716 repression and activation of the *tyrP* gene in *Escherichia coli*. J Bacteriol
717 173:5068–5078.
718 69. Leela JK, Syeda AH, Anupama K, Gowrishankar J. 2013. Rho-dependent
719 transcription termination is essential to prevent excessive genome-wide

R-loops in *Escherichia coli*. Proc Natl Acad Sci U S A110:258–263.

70. Raghunathan N, Goswami S, Leela JK, Pandiyan A, Gowrishankar J. 2019. A new role for *Escherichia coli* Dam DNA methylase in prevention of aberrant chromosomal replication. Nucleic Acids Res 47:5698–5711.
71. Ali N, Gowrishankar J. 2020. Cross-subunit catalysis and a new phenomenon of recessive resurrection in *Escherichia coli* RNase E. Nucleic Acids Res 48:847–861.
72. Dattananda CS, Rajkumari K, Gowrishankar J. 1991. Multiple mechanisms contribute to osmotic inducibility of proU operon expression in *Escherichia coli*: demonstration of two osmoresponsive promoters and of a negative regulatory element within the first structural gene. J Bacteriol 173:7481–7490.
73. Chang AC, Cohen SN. 1978. Construction and characterization of amplifiable multicopy DNA cloning vehicles derived from the P15A cryptic miniplasmid. J Bacteriol 134:1141–1156.
74. Dudas KC, Kreuzer KN. 2001. UvsW Protein regulates bacteriophage T4 origin-dependent replication by unwinding R-loops. Mol Cell Biol 21:2706–2715.
75. Carles-Kinch K, George JW, Kreuzer KN. 1997. Bacteriophage T4 UvsW protein is a helicase involved in recombination, repair and the regulation of DNA replication origins. EMBO J 16:4142–4151.
76. Wechsler JA, Gross JD. 1971. *Escherichia coli* mutants temperature-sensitive for DNA synthesis. Mol Gen Genet 113:273–284.
77. Dimude JU, Stockum A, Midgley-Smith SL, Upton AL, Foster HA, Khan A, Saunders NJ, Retkute R, Rudolph CJ. 2015. The consequences of replicating in the wrong orientation: bacterial chromosome duplication without an active replication origin. MBio 6:e01294-15.
78. Midgley-Smith SL, Dimude JU, Rudolph CJ. 2019. A role for 3' exonucleases at the final stages of chromosome duplication in *Escherichia coli*. Nucleic Acids Res 47:1847–1860.
79. Maduike NZ, Tehranchi AK, Wang JD, Kreuzer KN. 2014. Replication of the *Escherichia coli* chromosome in RNase HI-deficient cells: multiple initiation regions and fork dynamics. Mol Microbiol 91:39–56.

753 80. Wendel BM, Courcelle CT, Courcelle J. 2014. Completion of DNA
754 replication in *Escherichia coli*. Proc Natl Acad Sci U S A 111:16454–
755 16459.
756 81. Wendel BM, Cole JM, Courcelle CT, Courcelle J. 2018. SbcC-SbcD and
757 ExoI process convergent forks to complete chromosome replication. Proc
758 Natl Acad Sci U S A 115:349–354.
759 82. Azeroglu B, Mawer JS, Cockram CA, White MA, Hasan AM, Filatenkova
760 M, Leach DR. 2016. RecG Directs DNA Synthesis during Double-Strand
761 Break Repair. PLoS Genet 12:e1005799.
762 83. Harinarayanan R, Gowrishankar J. 2003. Host factor titration by
763 chromosomal R-loops as a mechanism for runaway plasmid replication
764 in transcription termination-defective mutants of *Escherichia coli*. J Mol
765 Biol 332:31–46.
766 84. Gowrishankar J, Harinarayanan R. 2004. Why is transcription coupled
767 to translation in bacteria? Mol Microbiol 54:598–603.
768 85. Gowrishankar J, Leela JK, Anupama K. 2013. R-loops in bacterial
769 transcription: their causes and consequences. Transcription 4:153–157.
770 86. Cardinale CJ, Washburn RS, Tadigotla VR, Brown LM, Gottesman ME
771 NE. 2008. Termination factor Rho and its cofactors NusA and NusG
772 silence foeign DNA in *E. coli*. Science 320:935–938.
773 87. Tan K, Zhou Q, Cheng B, Zhang Z, Joachimiak A, Tse-Dinh YC. 2015.
774 Structural basis for suppression of hypernegative DNA supercoiling by
775 *E. coli* topoisomerase I. Nucleic Acids Res 43:11031–11046.
776 88. Cao N, Tan K, Zuo X, Annamalai T, Tse-Dinh Y-C. 2020. Mechanistic
777 insights from structure of *Mycobacterium smegmatis* topoisomerase I
778 with ssDNA bound to both N- and C-terminal domains. Nucleic Acids
779 Res 48:4448–4462.
780 89. Miller JH. 1992. A Short Course in Bacterial Genetics: A Laboratory
781 Manual and Handbook for *Escherichia coli* and Related Bacteria. Cold
782 Spring Harb Lab Press NY.
783 90. Anupama K, Leela JK, Gowrishankar J. 2011. Two pathways for RNase
784 E action in *Escherichia coli* in vivo and bypass of its essentiality in
785 mutants defective for Rho-dependent transcription termination. Mol

786 Microbiol 82:1330-1348.
787 91. Gowrishankar J. 1985. Identification of osmoresponsive genes in
788 *Escherichia coli*: evidence for participation of potassium and proline
789 transport systems in osmoregulation. J Bacteriol 164:434–445.
790 92. Sambrook J, Russell D. 2001. Molecular Cloning: A Laboratory Manual.
791 3rd edn. Cold Spring Harb Lab Press NY.
792

Legends to figures

Figure 1. (A) Representations of *topA*$^+$ ORF delineating the encoded protein's domains D1 to D9 (adapted from 87, 88), and of the constructed *topA* alleles (three pairs) wherein the interrupted line segments represent deletions and each inverted triangle represents the pair comprising either Kan^R insertion (::Kan allele) or its FRT derivative (::FRT allele). **(B)** Blue-white screening assay on LB medium, of MG1655 or MDS42 strain derivatives with the *topA*$^+$ shelter plasmid pHYD2390 and the different *topA* alleles as indicated on the top of each column; the *rpoB* allele status is indicated at left of each row. Examples of white colonies are marked by the yellow arrows. From left to right, strains used for the panels were pHYD2390 derivatives of: row 1, GJ13519, GJ15603, GJ15604, GJ15688 and GJ16921; row 2, GJ16703, GJ16813, GJ16814, GJ16815 and GJ16854; row 3, GJ12134, GJ16816, GJ16817, GJ16818 and GJ18977; and row 4, GJ16819, GJ16820, GJ16821, GJ16822 and GJ17777.

Figure 2. Supercoiling status of reporter plasmid pACYC184 in *topA*$^+$ and *topA* derivatives, as determined by chloroquine-agarose gel electrophoresis. Genotypes at *topA* and *rpoB* loci are indicated on top of each lane; for *topA,* Δ and 480 refer, respectively, to Δ*topA*::FRT and *topA*-Ins480::FRT. Strains for different lanes were pACYC184 derivatives of: 1, GJ12134; 2, GJ16819; 3, 18976; 4, GJ18977; 5, GJ17776; 6, GJ17777; 8, GJ18601; and 9, GJ18910. Lane 7, DNA size standards.

Figure 3. Suppression of Δ*dnaA* lethality by *topA*. **(A)** Blue-white screening assay at 30° on glucose-minimal A with *topA*$^+$ *dnaA*$^+$ shelter plasmid pHYD2390 in MG1655 Δ*dnaA* Δ*tus rpoB*35* derivatives carrying different *topA* alleles; the nature of Δ*dnaA* allele (::Kan or ::FRT) and of *topA* allele are shown on top of each panel. Examples of white colonies are marked by the yellow arrows. Strains employed for the different panels were pHYD2390 derivatives of: i, GJ17786; ii, GJ17790; iii, GJ18940; iv, GJ17787; v, GJ17791; vi, GJ18941; vii, GJ17788; viii, GJ17792; and ix, GJ18942. **(B)** Serial dilution-spotting on LB and glucose-minimal A (MM) at indicated temperatures of the following derivatives of MG1655 Δ*tus rpoB*35*: Nil, *topA*$^+$ *dnaA*$^+$ (GJ17784/pHYD2390); *topA*, *topA*-Ins480::FRT *dnaA*$^+$ (GJ17784); and *topA*

825 *dnaA*, *topA*-Ins480::FRT Δ*dnaA*::FRT, that is, white colony from panel vi of
826 Figure 4A (GJ18941).

827 **Figure 4.** Copy number analysis by deep sequencing in *topA* mutant
828 derivatives of MDS42. In panels i to iv, relative copy numbers have been
829 plotted as semi-log graphs for overlapping 10-kb intervals across the genome
830 (relevant genotype of strain indicated on top of each panel); positions of *oriC,*
831 *TerA* and *TerC/B* are marked, and the gap at around 0.3 Mbp in each of the
832 plots corresponds to the *argF-lac* deletion present in the strains. Strains
833 displayed in the different panels are: i, GJ12134; ii, GJ16819; iii, GJ18977;
834 and iv, GJ17777.

835 **Figure 5.** Synthetic *topA rnhA* lethality, suppressed by Δ*dnaA*. Blue-white
836 screening assay at 30° on glucose-minimal A with *topA*$^+$ *dnaA*$^+$ shelter plasmid
837 pHYD2390 in MG1655 Δ*tus rpoB*35* derivatives carrying different alleles of
838 *topA*, *rnhA* and *dnaA* as indicated on top of each panel. Strains employed for
839 the different panels were pHYD2390 derivatives of: i, GJ17784; ii, GJ19609;
840 iii, GJ18951; iv, GJ17783; v, GJ19608; and vi, GJ18983.

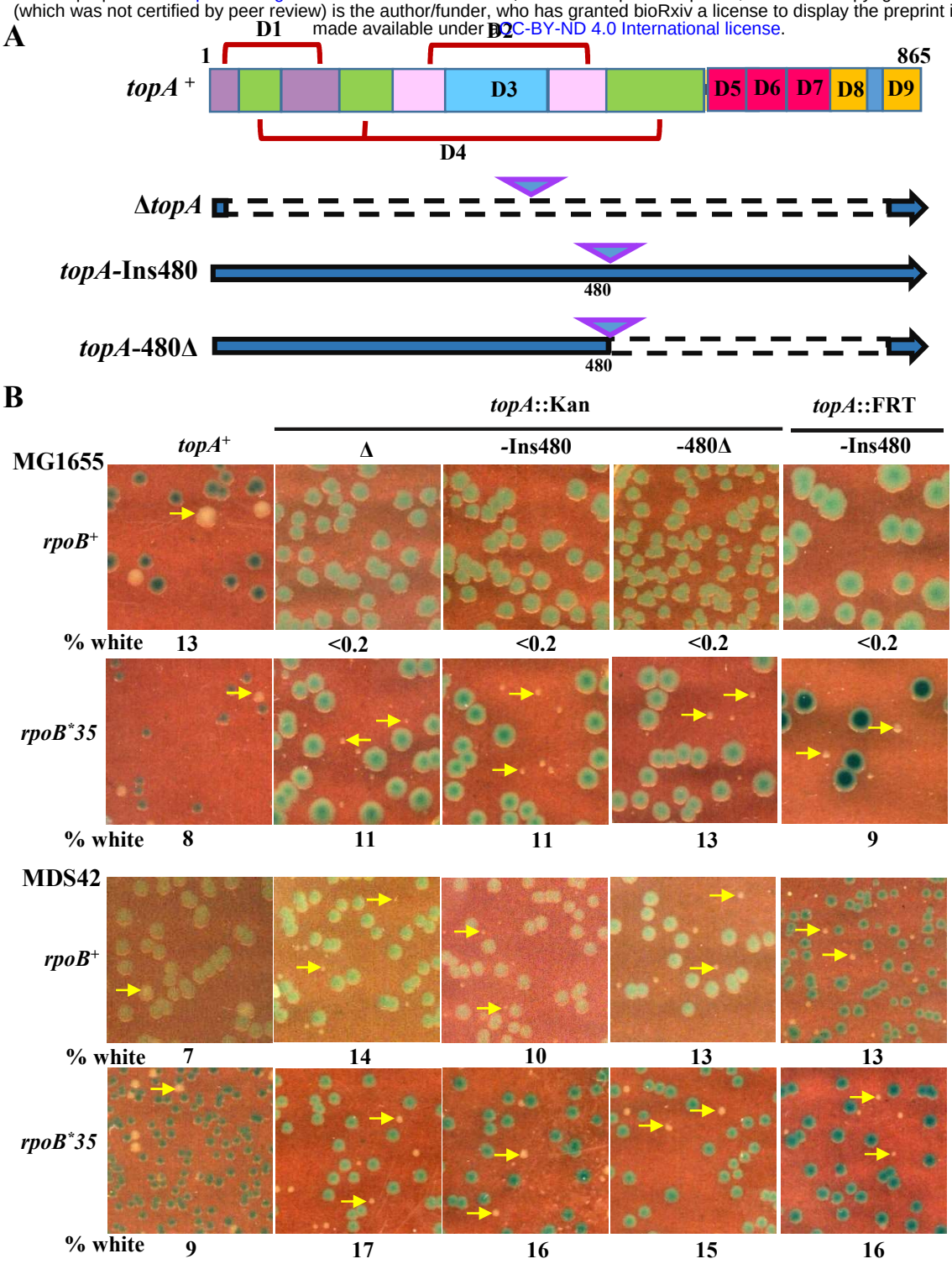

Figure 1. (A) Representations of *topA*$^+$ ORF delineating the encoded protein's domains D1 to D9 (adapted from 84, 85), and of the *topA* alleles (three pairs) constructed in this study wherein the interrupted line segments represent deletions and each inverted triangle represents the pair comprising either Kan^R insertion (::Kan allele) or its FRT derivative (::FRT allele). **(B)** Blue-white screening assay on LB medium, of MG1655 or MDS42 strain derivatives with the *topA*$^+$ shelter plasmid pHYD2390 and the different *topA* alleles as indicated on the top of each column; the *rpoB* allele status is indicated at left of each row. Examples of white colonies are marked by the yellow arrows. From left to right, strains used for the panels were pHYD2390 derivatives of: row 1, GJ13519, GJ15603, GJ15604, GJ15688 and GJ16921; row 2, GJ16703, GJ16813, GJ16814, GJ16815 and GJ16854; row 3, GJ12134, GJ16816, GJ16817, GJ16818 and GJ18977; and row 4, GJ16819, GJ16820, GJ16821, GJ16822 and GJ17777.

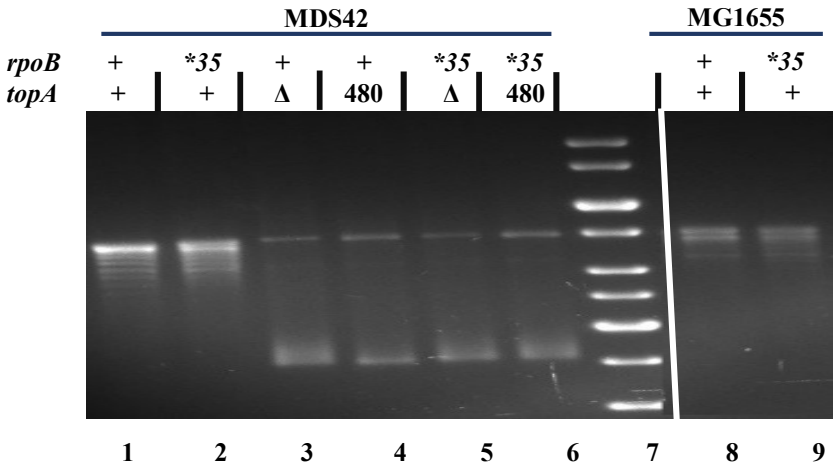

Figure 2. Supercoiling status of reporter plasmid pACYC184 in *topA*$^{+}$ and *topA* derivatives, as determined by chloroquine-agarose gel electrophoresis. Genotypes at *topA* and *rpoB* loci are indicated on top of each lane; for *topA*, Δ and 480 refer, respectively, to Δ*topA*::FRT and *topA*-Ins480::FRT. Strains for different lanes were pACYC184 derivatives of: 1, GJ12134; 2, GJ16819; 3, 18976; 4, GJ18977; 5, GJ17776; 6, GJ17777; 8, GJ18601; and 9, GJ18910. Lane 7, DNA size standards.

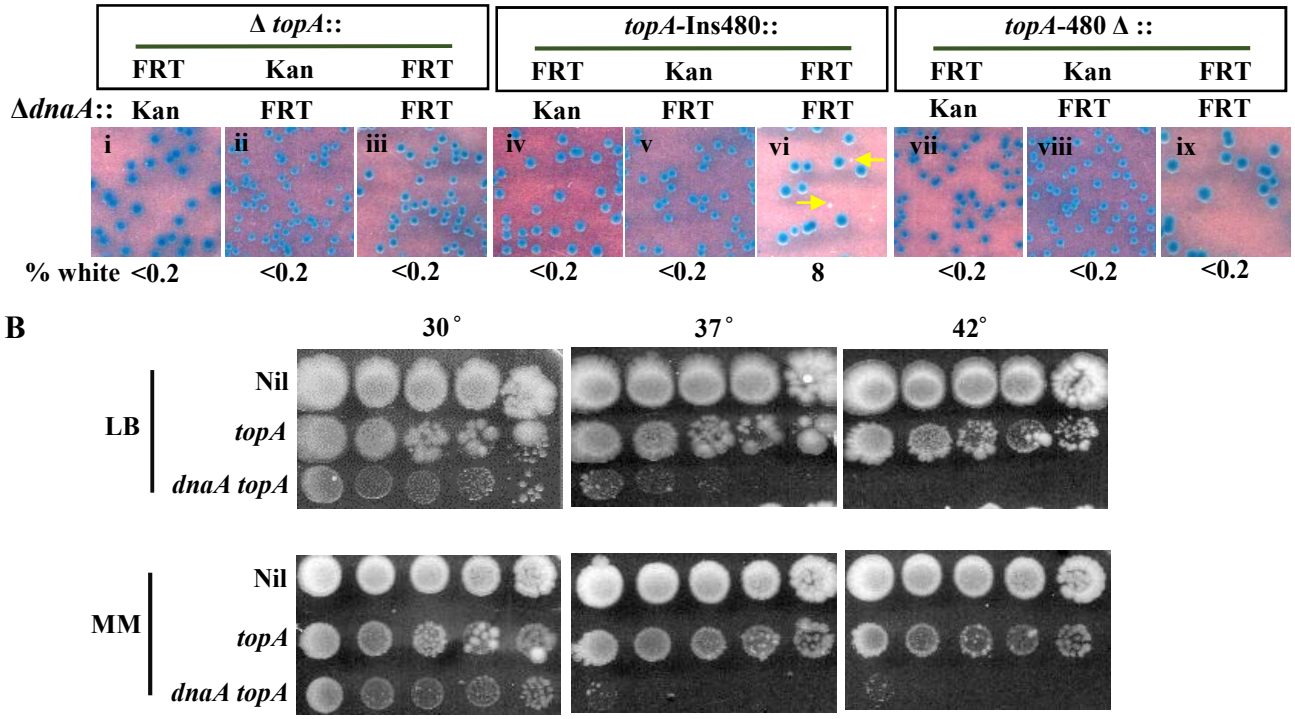

Figure 3. Suppression of Δ*dnaA* lethality by *topA*. **(A)** Blue-white screening assay at 30° on glucose-minimal A with *topA*$^+$ *dnaA*$^+$ shelter plasmid pHYD2390 in MG1655 Δ*dnaA* Δ*tus rpoB*35* derivatives carrying different *topA* alleles; the nature of Δ*dnaA* allele (::Kan or ::FRT) and of *topA* allele are shown on top of each panel. Examples of white colonies are marked by the yellow arrows. Strains employed for the different panels were pHYD2390 derivatives of: i, GJ17786; ii, GJ17790; iii, GJ18940; iv, GJ17787; v, GJ17791; vi, GJ18941; vii, GJ17788; viii, GJ17792; and ix, GJ18942. **(B)** Serial dilution-spotting on LB and glucose-minimal A (MM) at indicated temperatures of the following derivatives of MG1655 Δ*tus rpoB*35*: Nil, *topA*$^+$ *dnaA*$^+$ (GJ17784/pHYD2390); *topA*, *topA*-Ins480::FRT *dnaA*$^+$ (GJ17784); and *topA dnaA*, *topA*-Ins480::FRT Δ*dnaA*::FRT, that is, white colony from panel vi of Figure 4A (GJ18941).

Fig. 4

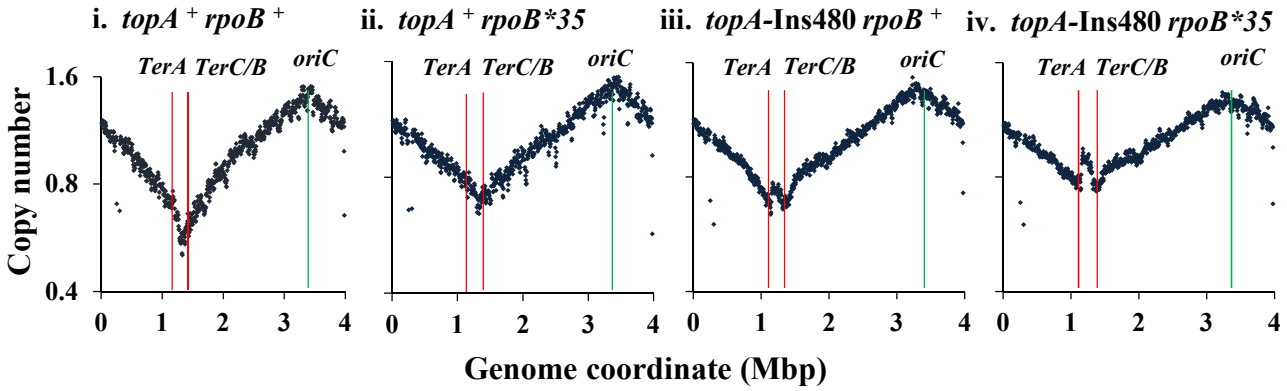

Figure 4. Copy number analysis by deep sequencing in *topA* mutant derivatives of MDS42. In panels i to iv, relative copy numbers have been plotted as semi-log graphs for overlapping 10-kb intervals across the genome (relevant genotypes of strain indicated on top of each panel); positions of *oriC, TerA* and *TerC/B* are marked, and the gap at around 0.3 Mbp in each of the plots corresponds to the *argF-lac* deletion present in the strains. Strains displayed in the different panels are: i, GJ12134; ii, GJ16819; iii, GJ18977; and iv, GJ17777.

Fig. 5

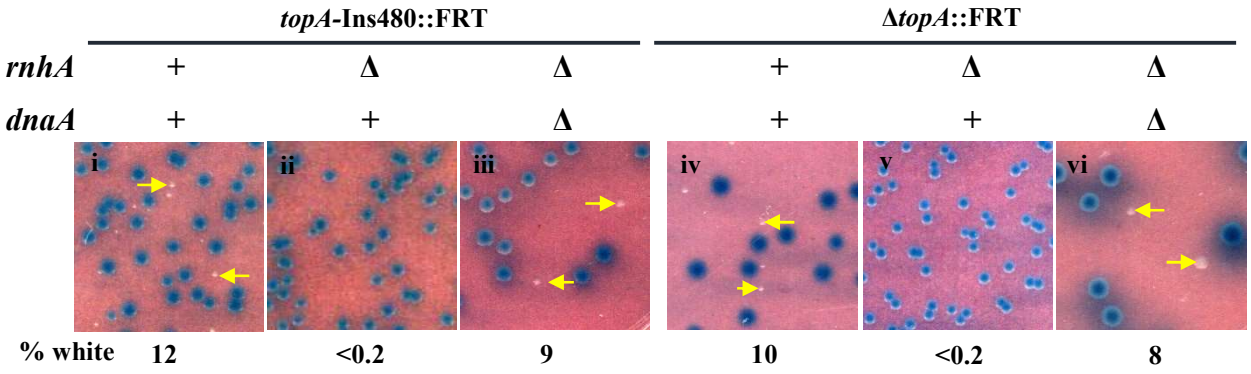

Figure 5. Synthetic *topA rnhA* lethality, suppressed by Δ*dnaA*. Blue-white screening assay at 30° on glucose-minimal A with *topA*$^+$ *dnaA*$^+$ shelter plasmid pHYD2390 in MG1655 Δ*tus rpoB*35* derivatives carrying different alleles of *topA*, *rnhA* and *dnaA* as indicated on top of each panel. Strains employed for the different panels were pHYD2390 derivatives of: i, GJ17784; ii, GJ19609; iii, GJ18951; iv, GJ17783; v, GJ19608; and vi, GJ18983.